International Journal of Computer Applications (0975 - 8887)
Volume 186 - No.15, April 2024

An EIT Data Acquisition System for Microtomography Applications

Adriano Regis
Mechatronics Engineering
Federal Institute of Santa Catarina,
Florianópolis, Brazil

Daniel J. Pagano
Department of Automation and Systems
Federal University of Santa Catarina
Florianópolis, Brazil

Francisco R.M. Mota
Mechatronics Engineering
Federal Institute of Santa Catarina,
Florianópolis, Brazil

ABSTRACT

Electrical Impedance Tomography is a soft-field technique able to generate images for several applications where a safe, non-intrusive and non-invasive approach is mandatory. This paper presents the study of a hardware implementation of an Electrical Impedance Tomography System, suitable for data acquisition and image reconstruction to microtomography applications, characterizing MicroEIT in the context of the different applications of existing tomography techniques, as well as highlights the temporal problem encountered in the approaches already developed. The concepts and elements of a MicroEIT system are shown in a proposal of hardware and software implementation using our measurement and excitation hardware, integrated to a CompactRIO and LabVIEW data acquisition system. Finally, it discusses the possibility of applications of this approach in cell culture studies.

General Terms

Electrical impedance tomography, Microtomography

Keywords

Hardware implementation, microsensor, microtomography, Labview instrumentation

1. INTRODUCTION

Tomography is a method capable of producing internal images of objects by observing the passage of different types of energy waves through their structures. Due to its non-invasive nature, tomography is applied in several areas of knowledge, such as Geology, Industrial Processes and Medicine [11].

X-ray tomography, widely used in the medical field, is a hard-field technique that uses electromagnetic waves between $\lambda = 1 \times 10^{-8} m$ and $\lambda = 1 \times 10^{-12} m$ in which the pixels of the generated image are directly proportional to the intensity of the direct radiation beam [7]. The use of this spectrum range is justified by the hard-field technique because, if the radiation occurs at lower frequencies in the spectrum, scattering effects would need to be taken into account. Although the principle of image construction using these techniques is relatively simple, the volume, complexity, costs and security aspects of such equipment are restrictive factors for their application in certain contexts. At lower frequencies, the *nonlocal* property of the conductivity image demands a system of equations able to relate each pixel of the image to the measurements, therefore requiring a relative computational processing power in image reconstruction and a particular treatment of emitting signals and receptors in obtaining readings. The possible difficulties that exist, in terms of measuring and processing images at these frequencies are, to a certain extent, compensated with the inherently non-intrusive advantages or mitigated by technological advances in the areas of hardware and software [11]. These advances have allowed the establishment of a series of soft-field tomography techniques, such as the well-known electrical tomography techniques, among which are (i) Electrical Capacitance Tomography, (ii) Magnetic Induction Tomography and (iii) Electrical Resistance Tomography.

A particular technique of tomography based on electrical principles is called Electrical Impedance Tomography–EIT, which considers the resistive and reactive aspects of the materials arranged in the area of interest, simultaneously obtaining data corresponding to the electrical properties of conductivity and permittivity, therefore, this is a technique based on the spatial distribution of electrical admittance.
As a technique based on resistive and reactive properties of materials, EIT has a hybrid set of characteristics in terms of application. Table 1 shows how EIT is related to other tomography methods based on electrical principles.

1.1 MicroEIT

As shown in Table 1, the particular characteristics of EIT make it applicable to the analysis of biological systems and, therefore, it is worth highlighting the potential use of the so-called microEIT [9] or Microimpedance [6] in obtaining images at a microbiological level. In studies with cell cultures, for example, it is possible to obtain experimental data under conditions unattainable by traditional observational methods.

As highlighted by Lei [4], the conventional microscopy approach adopted in cell cultures, based on counting, quantification of components and metabolic analysis, is laborious and time-consuming, limiting the testing of drugs and toxins. Furthermore, cellular indicators are intrusive and, in many cases, destructive methods to the point of making analysis of the cellular response subsequent to observation unfeasible. The use of cell cultures in cellular drug re-

Table 1. Comparison between the different tomography techniques based on electrical principles

Feature	Resistive	Capacitive	Inductive	Impedance
Elements	Electrodes	Electrodes	Coils	Electrodes
Electrode/electrolyte	With contact	Without contact	Without contact	With contact
Main use	Ionized solutions	Deionized solutions	Metal alloys	Biological tissues

Characteristics of tomography methods based on electrical principles.

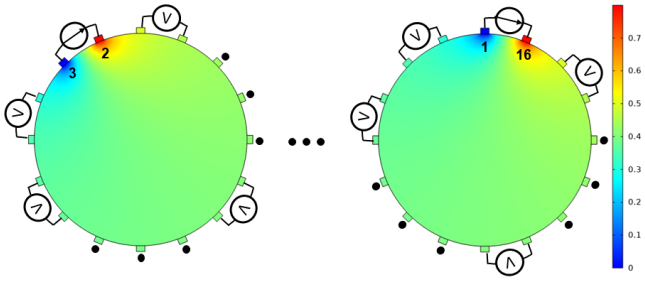

Fig. 1. Representation of the adjacent excitation/measurement protocol implementation

search or bone tissue regeneration, for example, requires the use of non-intrusive techniques with high temporal resolution to monitor transient cellular activities.

2. THE GENERAL CONFIGURATION OF EIT SYSTEMS

Since the development of the first EIT system by Barber and Brown [1], a considerable number of publications have been carried out in different areas of application. However, whatever the application, an EIT system is basically composed of two blocks: hardware and software. The hardware block consists of a Sensor and a Control and Acquisition Unit. Depending on the application, the Sensor can be manufactured in circular or planar electrode arrays in single (2D applications) or multilayer (3D applications). In the Control and Acquisition Unit, the generation, adaptation/conversion and management of the excitation signal for the emitting electrodes and the acquisition of the measured signals (coming from the electrodes) take place.

Excitation and measurement management is commonly called the excitation/measurement protocol, with the Adjacent/Neighbor Protocol (Fig. 1) being the most commonly used. In this protocol, a pair of adjacent electrodes (or neighbors) is used as a current emitter, while the other adjacent pairs are used to measure voltage; each of the electrodes must (at least once) act as a transmitter and, therefore, the total number of measurements will be $m = n \cdot (n - 3)$, where m corresponds to the total number of measurements and n corresponds to the number of electrodes.

3. INVERSE PROBLEM

In EIT applications, the inverse problem consists of determining the conductivity distribution γ from the voltage values V_l measured at the electrodes. To reconstruct the conductivity distribution (image), the Difference Method is usually adopted. Such a method determines the permittivity distribution based on the difference between measured data and reference data.

Adopting the equation developed by Rimpiläinen [8] and adapting it to EIT, obtain

$$I_l(\gamma) \approx I_l(\gamma_{lin}) + \sum_{i=1}^{n} \frac{\partial I_l}{\partial \gamma_i}(\gamma_i - \gamma_i^{lin}) \tag{1}$$

where γ_i^{lin} is the conductivity without equilibrium point and n represents the number of elements used to discretize.
The first equation was obtained by linearizing the electrode current to the equilibrium point γ_{lin} and neglecting the higher order terms resulting from the Taylor series approximation. When the same approximation is applied to all currents, the matrix equation is obtained

$$I(\gamma) \approx I(\gamma_{lin}) + \mathbf{S}(\gamma - \gamma_{lin}) \tag{2}$$

Likewise, the equation of the voltage observation can be approximated by

$$V \approx \phi(\gamma_{lin}) + \mathbf{S}(\gamma - \gamma_{lin}) + v_v \tag{3}$$

$$V_{ref} \approx \phi(\gamma_{lin}) + \mathbf{S}(\gamma_{ref} - \gamma_{lin}) + v_{v,ref} \tag{4}$$

By subtracting the Eq.4 of Eq.3 and adopting $\lambda = V - V_{ref}$, $\mathbf{g} = \gamma - \gamma_{ref}$ e $\delta v_v = v_v - v_{v,ref}$, can be write the (2) as

$$\lambda \approx \mathbf{S}\mathbf{g} + \delta v_v \tag{5}$$

where $\mathbf{S}$ represents the Jacobian matrix (or sensitivity matrix) given by

$$\mathbf{S}_{m\times n} = \begin{bmatrix} \frac{\partial V_1}{\partial \gamma_1} & \frac{\partial V_1}{\partial \gamma_2} & \cdots & \frac{\partial V_1}{\partial \gamma_n} \\ \frac{\partial V_2}{\partial \gamma_1} & \frac{\partial V_2}{\partial \gamma_2} & \cdots & \frac{\partial V_2}{\partial \gamma_n} \\ \vdots & \vdots & \ddots & \vdots \\ \frac{\partial V_m}{\partial \gamma_1} & \frac{\partial V_m}{\partial \gamma_2} & \cdots & \frac{\partial V_m}{\partial \gamma_n} \end{bmatrix} \tag{6}$$

where m and n represent the measurement number and the number of elements used in the discretization, respectively.
Thus, it can be said that solving the inverse problem consists of solving (3) for $\mathbf{g}$. As presented in [7], Landweber's iterative method can be used to approximate $\mathbf{g}$.
Landweber's algorithm is a variant of the gradient descent method (*steepest descent* or *gradient descent*) and was originally developed to solve the least squares problem. The algorithm minimizes the following objective function [3]; [5].

$$\min f(\mathbf{g}) = \frac{1}{2}\|\mathbf{S}\mathbf{g} - \lambda\|^2 \tag{7}$$

With $f(\mathbf{g})$ given by

$$f(\mathbf{g}) = \frac{1}{2}(\mathbf{S}\mathbf{g} - \lambda)^T(\mathbf{S}\mathbf{g} - \lambda) = \frac{1}{2}(\mathbf{g}^T\mathbf{S}^T\mathbf{S}\mathbf{g} - 2\mathbf{g}^T\mathbf{S}^T\lambda + \lambda^T\lambda) \tag{8}$$

the gradient of $f(\mathbf{g})$ can be calculated as

$$\nabla f(\mathbf{g}) = \mathbf{S}^T\mathbf{S}\mathbf{g} - \mathbf{S}^T\lambda = \mathbf{S}^T(\mathbf{S}\mathbf{g} - \lambda) \quad (9)$$

The gradient descent method chooses the direction in which $f(\mathbf{g})$ decreases fastest as the new direction for the next iteration. This direction is opposite to the gradient of $f(\mathbf{g})$ at the current point. The iteration procedure is therefore

$$\hat{\mathbf{g}}_{k+1} = \hat{\mathbf{g}}_k - \mu_k \nabla f(\hat{\mathbf{g}}_k) = \hat{\mathbf{g}}_k - \mu_k \mathbf{S}^T(\mathbf{S}\hat{\mathbf{g}}_k - \lambda) \quad (10)$$

where the term $\mu_k\mathbf{S}^T$ represents the initial approximation of $\mathbf{S}^{-1}$ and μ_k, called the relaxation factor (or gain factor), is a positive scalar that defines the size of the iteration step (*step size*). A simple way to choose μ_k is to assign it a fixed value at the beginning of the iterative process. For fixed μ_k, Landweber's algorithm can be expressed as

$$\hat{\mathbf{g}}_{k+1} = \hat{\mathbf{g}}_k - \mu\mathbf{S}^T(\mathbf{S}\hat{\mathbf{g}}_k - \lambda) \quad (11)$$

The value of μ_k can also be defined based on a certain convergence criterion. For example

$$\|\mu\mathbf{S}^T\mathbf{S}\|_2 < 2 \quad (12)$$

Thus, μ can be given by

$$\mu = \frac{2}{\delta_{max}} \quad (13)$$

where δ_{max} is the maximum eigenvalue of $\mathbf{S}^T\mathbf{S}$.
In Eq. 10, the term $\hat{\mathbf{g}}_k$ represents the initial solution, which can be equal to zero or obtained, for example, by a direct algorithm such as Linear Backprojection (*Linear Back-projection - LBP*. When $\hat{\mathbf{g}}_k$ is assigned a value equal to zero, the solution converges to the minimum norm least squares solution [10].

4. HARDWARE ARCHITECTURES FOR MEASUREMENT AND EXCITATION

An EIT system can obtain the impedance distribution pattern through a tetrapolar arrangement injecting current between a given pair of electrodes and measuring voltages between pairs of neighboring electrodes, using one or more current sources and one or more voltage measurement systems.

It is possible to observe that most EIT systems are based on hardware architectures in which a single current source and voltage measurement system are responsible for the impedance distribution pattern. This is possible thanks to the adoption of a switching protocol for electrode selection and, as shown in Fig. 2 , these systems use switching devices to implement the switching of current injection and voltage measurement over time.

4.1 Proposed approach

To collect experimental data, a specific hardware and software prototype was designed and built for microtomography applications, where the hardware block consists of a Compact DAQ chassis (NI 9188), the sensor and developed hardware that includes most of the embedded subsystems and the software implemented in Labview, as can be seen in the block diagram of Fig. 3 .

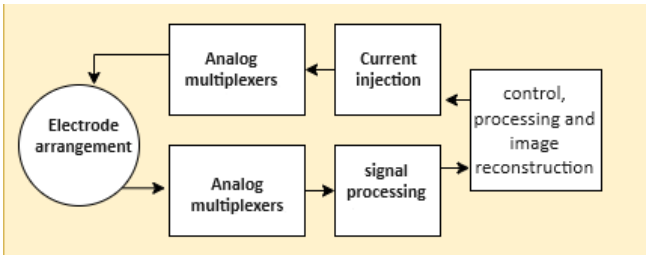

Fig. 2. Block diagram of an excitation and measurement architecture in EIT system

5. HARDWARE DETAILS

The proposed hardware, called the mEIT prototype, was distributed in three Printed Circuit Boards-PCB, whose design in a CAD environment as shown in (Fig. 4) (Fig. 5) shows a picture of the real prototype.. The project provides for the interconnection between the PCBs through a standard bus, which allows the inclusion of new expansion boards for concept tests to be developed in the continuity of the research.

In terms of subcircuits, the project includes:

(1) a constant current source;

(2) a multiplexing module;

(3) a planar micro-sensor;

(4) a signal conditioning subcircuit.

5.1 The Current source subcircuit

Considering the needs of non-intrusive and/or invasive, current sources for EIT systems applied to bioimpedance are inherently characterized as low-power systems. These sources are implemented through various circuits such as Howland Bridge and Transconductance Operational Amplifiers [2]. However, considering the particular characteristics for measurement in microTIE, this prototype uses an excitation signal subcircuit based on a voltage-controlled current source, which converts the sinusoidal signal coming from the internal DDS circuit into a constant current signal by means of a Precision Differential Gain Amplifier.

The current used in this system is, therefore, less than 1.5mA RMS.

5.2 The multiplexing subcircuit

The switching of the injection and measurement electrodes was implemented through four integrated 16-channel bidirectional analog multiplexing circuits model CD74HC4067. The multiplexing of the two signals from the excitation circuit, as well as the two differential inputs from the measurement circuit, occurs with different pairs of components, which makes it possible to reduce any parasitic capacitance in the system.

The component used has electrical characteristics that satisfy the project demands such as low contact impedance (70 ohms typical), low noise and high switching speed.

The addressing of the inputs allows the switching protocol that is carried out by the NI-9403 Digital Inputs and Outputs module connected to the Compact DAQ Chassis.

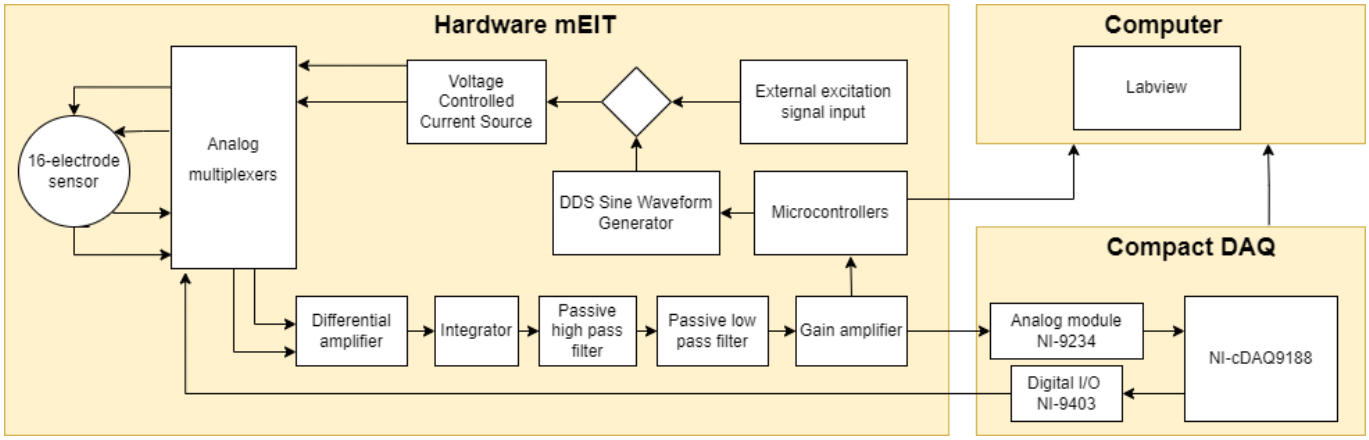

Fig. 3. Block diagram of the proposed system

5.3 Microsensor EIT

The EIT microsensors were built with planar electrodes on a Printed Circuit Board due to the ease of manufacturing using techniques already consolidated by the electronics industry. The developed mEIT consists of an array of 16 flat copper electrodes arranged radially on a PCB laminate with fiberglass insulation and reinforced with Epoxy-FR.4.. The total diameter of the sensor corresponds to 15.5 mm, while each rectangular electrode has dimensions of 1.7 mm x 0.8 mm.

The electrode area is confined by a transparent acrylic tube with an internal diameter of 15 mm, 2 mm thick and 10 mm high. The microsensor is connected to the rest of the hardware using a single-in-line connector bus.

5.4 Signal conditioning subcircuit

The voltage from the measuring electrodes is sending to a multistage subcircuit responsible for conditioning the signal obtained for the respective A/D conversion, in this case, carried out by the NI-9234 external module integrated into the Compact DAQ Chassis.

The first stage of the proposed system consists of an AD620 Instrumentation Amplifier whose input impedance characteristics and common mode rejection bandwidth meet the design characteristics. The output of this first stage is coupled to an integrator block which, in turn, feeds back to the AD620 Instrumentation Amplifier at its reference input, removing the DC components from the signal. This step is necessary to guarantee the effective resolution of the A/D conversion steps.

The signal goes to a passive series bandpass circuit, whose bandwidth is between 0.7Hz and 117kHz, thus eliminating high frequency noise or any DC components not removed by the integrator circuit in the previous step. Finally, the filtered signal without DC component is amplified in a simple non-inverting configuration, allowing the entire A/D conversion range of the next step to be explored. The output of this subcircuit is available on a BNC connector for external connection to the NI-9234 module, integrated into the Compact DAQ Chassis.

The developed hardware also has an onboard symmetric power supply to provide energy to all components of this subcircuit.

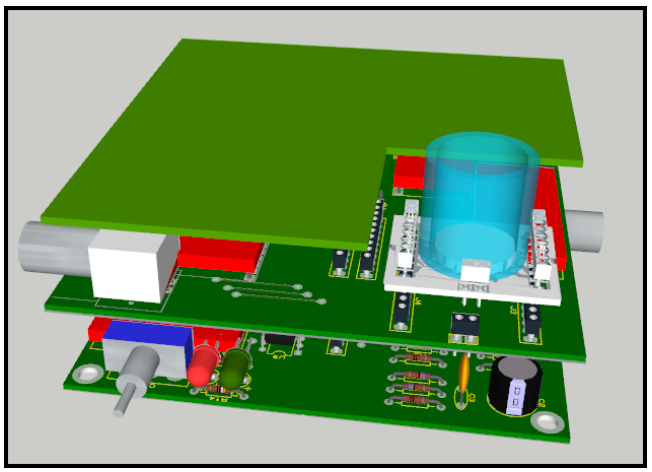

Fig. 4. Rendering of the prototype in Computer Aided Design system

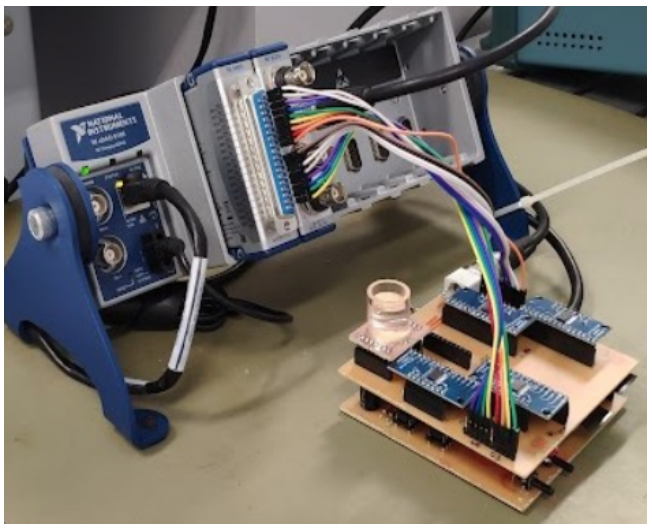

Fig. 5. Real assembly of the prototype

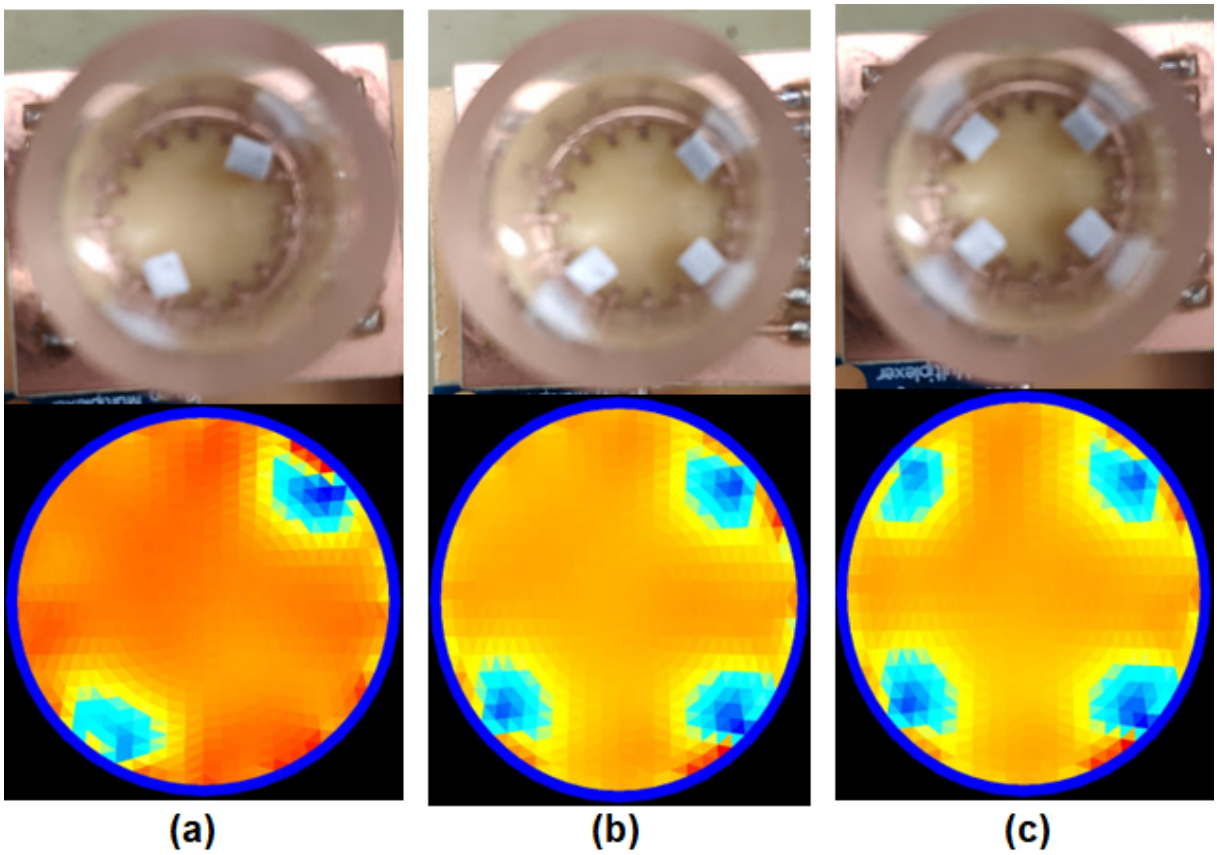

Fig. 6. Result of the image reconstruction with two (a) three (b) and four (c) pellets

6. SOFTWARE FOR SWITCHING CONTROL AND RECONSTRUCTION OF IMAGE

The software block was implemented using the LabView platform and is composed of the illustrated command sub-blocks, acquisition and conditioning; voltage calculation; conductivity calculation (implementation of the Landweber iterative algorithm) and image reconstruction.

The Command, Acquisition and Conditioning sub-block is responsible for sending command signals to the multiplexers, controlling which electrodes are in transmitter mode and which are in receiver mode (according to adjacent protocol). It is also responsible for acquiring signals from the measurement circuit. A case structure was created to generate the command sequence for the m = 208 measurements. A loop structure and an iteration counter were used to increment the control bit of the case structure until 208 measurements were performed. After each sequence of commands, the voltage value is acquired, and the RMS value is obtained using LabView's RMS PtByPt function.

The Voltage Calculation sub-block is executed sequentially to the previous sub-block. The value λ is calculated by performing the subtraction between the measured voltage vector (V) and the reference voltage vector (Vref) previously stored.

The Conductivity Calculation and Image Reconstruction sub-block is executed sequentially to the previous sub-block. The vector λ, together with the sensitivity matrix (S, previously archived), are used as input for the Landweber algorithm which will result in the conductivity vector (g).

Finally, to represent the conductivity distribution in an image, Labview's 3D Picture Control toolbox was used. Conductivity values were normalized and converted to RGB values.

7. TEST BENCH

The hardware and software developed for image reconstruction were evaluated by carrying out experiments in which the microsensor was filled with salline water and Acrylonitrile Butadiene Styrene pellets were positioned. in the area of interest. Fig. 6 shows the result of image reconstruction in three tests with a) two pellets; b) three pellets and c) four pellets. The electrodes was stimulated using the adjacent protocol with an alternating current of approximately 252 microampers and a frequency of 2.005kHz, resulting in 208 measurements per image. The average time for each test was approximately 10 minutes.

8. CONCLUSIONS

This paper addressed the study and development of a hardware setup applied to microEIT. The hardware of the proposed system was building taking into account the use of computer simulations as well as the implementation of diverse functional prototypes in order to obtain real performance results. The design performance

in terms of image resolution, time response and signal noise ratio in microparticle measurement and excitation tests states that the proposed solution can be used in future experiments applied in microtissues, such as *in vivo* cell cultures, drug experiments, and similar. It should be noted that in addition to the optimal performance of the hardware solution, the subcircuits were based on low-cost and widely accessible technologies, which became a promising approach. The software solution, entirely based on the Labview programming language, shows the viability of this environment in EIT research. Future research in terms of hardware and software improvements should focus on reducing measurement time in order to provide a real-time imaging system for the mentioned applications.

9. REFERENCES

[1] D. C. Barber and B. H. Brown. Applied potential tomography. *Journal of the British Interplanetary Society*, 42(7):391–393, 1989.

[2] Pedro Bertemes-Filho, Volney C. Vincence, Marcio M. Santos, and Ilson X. Zanatta. Low power current sources for bioimpedance measurements: A comparison between Howland and OTA-based CMOS circuits. *Journal of Electrical Bioimpedance*, 3(1):66–73, 2012.

[3] Lei Jing, Shi Liu, Li Zhihong, and Sun Meng. An image reconstruction algorithm based on the extended Tikhonov regularization method for electrical capacitance tomography. *Measurement: Journal of the International Measurement Confederation*, 42(3):368–376, 2009.

[4] Kin Fong Lei. Review on impedance detection of cellular responses in micro/nano environment. *Micromachines*, 5(1):1–12, 2014.

[5] Yan Li, Shuai Cao, Zhiqiang Man, and Huanhuan Chi. Image reconstruction algorithm for electrical capacitance tomography. *Information Technology Journal*, 10(8):1614–1619, 2011.

[6] Pontus Linderholm, Laurent Marescot, Meng Heng Loke, and Philippe Renaud. Cell culture imaging using microimpedance tomography. *IEEE Transactions on Biomedical Engineering*, 55(1):138–146, 2008.

[7] F. R. M. Mota. *Capacitive Tomometry applied to the measurement of water fraction in two-phase flows*. PhD thesis, UFSC, 2015.

[8] Ville Rimpiläinen. *Electrical Tomography Imaging in Pharmaceutical Processes*. PhD thesis, University of Eastern Finland, 2012.

[9] Hancong Wu. *Electrical impedance tomography for real-time 3D tissue culture monitoring*. PhD thesis, The University of Edinburgh, 2020.

[10] W Q Yang, D M Spink, T A York, and H McCann. An image-reconstruction algorithm based on landweber's iteration method for electrical-capacitance tomography. *Measurement Science and Technology*, 10(11):1065–1069, 1999.

[11] Trevor York. Status of electrical tomography in industrial applications. *Journal of Electronic Imaging*, 10(3):608, 2001.